



ENHANCED SATURATION OF LIQUID-SATURATED POROUS MEDIUM WITH ATMOSPHERE GASES DUE TO SURFACE TEMPERATURE OSCILLATIONS

D.S. Goldobin¹ and A.V. Dolmatova^{1,2}

¹*Institute of Continuous Media Mechanics UB RAS, Perm, Russian Federation*

²*Institute for Information Transmission Problems of RAS, Moscow, Russian Federation*

We study the non-isothermal diffusion transport of a poorly soluble substance in a porous liquid-saturated medium being in contact with the reservoir of this substance. The surface temperature of a half-space porous medium oscillates in time, which creates a decaying temperature wave propagating deep into sediments. Since the solubility exponentially strongly depends on temperature, a decaying running solubility wave forms in the porous medium. In such a system, the zones of saturated solution and non-dissolved phase coexist with the zones of undersaturated solution. The effect is considered for the case of annual oscillation of the surface temperature of water-saturated ground being in contact with atmosphere. We reveal the phenomenon of formation of a near-surface bubbly horizon due to the temperature oscillation for one- and two-component solutes. In the case of a two-component solute, the solubility depends on the composition of the nondissolved phase, which necessitates the construction of a corresponding mathematical model of dissolution of multicomponent mixtures. We develop an analytical theory of the phenomenon of formation of the bubbly horizon. In both analytical theory and numerical simulations, the temperature dependence of the molecular diffusion coefficient is taken into account. In the presence of a propagating temperature wave, the nonlinear interaction between this dependence and the temperature dependence of the solubility creates an additional nonzero contribution to the mean-over-period mass flux. For multicomponent solutions, we report the formation of a diffusive boundary layer, which is not possible for single-component solutions. We construct an analytical theory for this boundary layer and derive effective boundary conditions for the problem of the diffusive transport beyond this layer. Theoretical results are in fair agreement with the results of numerical simulation.

Key words: diffusion transport, porous media, solubility of atmosphere gases

1. Introduction

The process of diffusion transfer in bubbly media [1–6] and media with a condensed insoluble phase [3, 7–9] is of particular interest because it reveals unique features both in isothermal and nonisothermal conditions. In such systems, the insoluble phase makes the local solute concentration equal to the solubility. The concentration of the dissolved substance is no longer a “free” variable, but it becomes a function of temperature and pressure. At the same time, the nonzero divergence of the solute flux due to the solubility gradient does not change the concentration of the trapped solute, but redistributes the mass of the insoluble phase. Thus, in determining the dynamics of systems with an insoluble phase new phenomena and mechanisms come into play that never occur in undersaturated solutions. They are especially pronounced in systems in which the undissolved phase is immobilized (for example, captured in a porous medium), provided that the solubility is low [4]. For the immobilized insoluble phase, mass transfer occurs only through the solution and, when the solubility is low, the mass accumulated in the insoluble phase can be several orders of magnitude greater than the dissolved mass.

The influence of surface temperature fluctuations, which creates a solubility wave, on diffusion transfer in a porous medium, where the undissolved phase is present everywhere, was shown in [5]. However, systems where undissolved phase zones can coexist with unsaturated solution zones, demonstrate essentially more complex dynamics. A porous medium saturated with a liquid in contact with a large volume of a weakly soluble substance (e.g., with the atmosphere) is a striking example of such a system. In this paper, we consider the effect of surface temperature oscillations on diffusion transfer in a half-space of a porous medium in contact with a large volume of a weakly soluble substance.

From the mathematical point of view, the contact with the atmosphere is taken into account through the boundary condition, according to which the concentration of the dissolved substance at the contact boundary is assumed to be equal to the solubility at any time. In this paper, it will be shown that the temperature wave leads to the formation of a near-surface bubble horizon and oversaturation of the medium with atmospheric

gas compared to the period average solubility. In particular, the net mole fraction (undissolved phase + solution) of gas molecules in the pores near the surface is equal to the maximum solubility for the period.

The described phenomenon is important for systems with different origins of surface temperature fluctuations, including technological systems (filters, porous bodies of nuclear and chemical reactors, and others). However, for the sake of certainty, let us focus on the case characterized by a hydrostatic pressure gradient, since this is the state of geological systems in which pressure doubles at a depth of 10 meters, which leads to a significant change in solubility.

The effect of enhanced filling of the water-saturated soil with atmospheric gases creates more favorable conditions for local flora and fauna and affects the conditions of many geochemical processes. Thus, methane gas is released from methane hydrate deposits in the bottom sediments of water bodies under the influence of temperature waves, which is of interest in the context of natural Glacial cycles [10] and potential global climate change [11].

2. Diffusion in saturated multi-component solutions

2.1. Physical and mathematical models

The problem under consideration is conveniently described in terms of the molar concentration of the dissolved substance, which is the amount of solute per 1 mole of solvent. For a one-component ideal gas in thermodynamic equilibrium, the molar solute concentration in contact with the gas phase (solubility) is determined according to the Henry's law [12];

$$P = K_H X_s^{(0)}, \quad (1)$$

where P is the pressure and K_H is the Henry's law constant. According to the scale particle theory [13],

$$K_H = \frac{P_0}{X_s^{(0)}(T_0, P_0)} \frac{T}{T_0} \exp \left[q \left(\frac{1}{T_0} - \frac{1}{T} \right) \right]. \quad (2)$$

Here T is the temperature; T_0 and P_0 are the reference values (their choice is determined solely by the convenience of calculations); $X^{(0)}(T_0, P_0)$ is the solubility at reference temperature and pressure; the parameter $q \equiv -G_i/k_B$, where G_i is the interaction energy of the solute molecule with the surrounding solvent molecules, and k_B is the Boltzmann constant, is provided in the Table for several typical gases. The scaling particle theory makes it possible to find q and $X^{(0)}(T_0, P_0)$ from the first principles, while equation (2) is more general. With empirically determined q and $X^{(0)}(T_0, P_0)$, equation (2) is applicable for moderate fluctuations in temperature and pressure, at which the gas can be considered ideal (usually at pressures of up to several tens of atmospheres).

In multicomponent gases, each gas component in the solution creates a partial pressure P_j in the gas phase according to

$$P_j = K_{H,j}(T) X_{s,j}, \quad (3)$$

where $K_{H,j}$ is the Henry's law constant of specie j , $X_{s,j}$ is the concentration of the solution of specie j . For the molar fraction Y_j of the j -th component in the gas,

$$P_j = P Y_j,$$

and pressure $P = \sum_j P_j$. Thus, $\sum_j Y_j = 1$.

Under normal conditions, the solubility of typical gases (see Table) is so low that when the dissolved molecules form gas bubbles, the volume fraction of these bubbles in the liquid inside the pores will be negligibly small. Consequently, it is convenient to quantify the composition of the liquid in the pores using

$X_{s,j}$, $X_{b,j}$ and $X_{\Sigma,j} = X_{s,j} + X_{b,j}$, where $X_{s,j}$ is the number of molecules j in the solution divided by the total number of molecules in the liquid and gas phases, $X_{\Sigma,j}$ is the number of molecules j in the gas phase (bubbles) divided by the total number of molecules, and $X_{s,j}$ is the net molar fraction of the substance in the liquid inside the pore. Since the volume fraction of the gas phase in the pores is small, $X_{s,j}$ is almost equal to the molar solute concentration, the quantitative discrepancy between $X_{s,j}$ and the corresponding molar concentration can be neglected.

Table. Chemical physical properties of solutions of nitrogen, oxygen, methane and carbon dioxide in water

Component	N ₂	O ₂	CH ₄	CO ₂
Parameter				
$q = -G_i/k_B, K$	781	831	1138	1850
$X^{(0)} \times 10^5 (20^\circ C, 1 \text{ atm})$	1,20	2,41	2,60	68,7
$R_d \times 10^{10}, m$	1,48	1,29	1,91	1,57
$\nu \times 10^5, Pa \cdot c$	9,79	16,3	28,3	4,68

Note: Equations (1), (2) with the values q and $X^{(0)}(T_0, P_0)$ are correspond to the experimental data from [14–16].

2.1.1. Solubility of two-component gas

Let us consider a two-component gas. Such a problem is especially relevant for modeling the Earth's atmosphere, where nitrogen and oxygen make up 99% of the entire molar composition. If the composition of the liquid in the pores ($X_{\Sigma,1}$ and $X_{\Sigma,2}$) is known, one can estimate whether a gas phase will form, and calculate the composition of the solution and the gas phase. For the gas phase formation, the maximum solute concentrations $\max(X_{s,j}) = X_{\Sigma,j}$ must be sufficient to create a vapor pressure exceeding the pressure $\max(P_1 + P_2)$. According to equation (3), the condition for the gas phase formation is

$$K_{H,1}X_{\Sigma,1} + K_{H,2}X_{\Sigma,2} > P. \tag{4}$$

When the gas phase forms, its equilibrium composition is determined by Eq. (3);

$$K_{H,j}X_{s,j} = PY_j \tag{5}$$

and

$$X_{s,j} + X_{b,j} = X_{\Sigma,j}, \tag{6}$$

$$X_{b,1}/X_{b,2} = Y_1/Y_2, \tag{7}$$

$$Y_1 + Y_2 = 1. \tag{8}$$

With $j=1,2$, the system (5)–(8) gives six equations for six unknowns $X_{s,j}$, $X_{b,j}$, Y_j and has a unique solution

$$X_{s,1} = \frac{2X_{\Sigma,1}X_{s,1}^{(0)}}{X_{\Sigma,1} + X_{\Sigma,2} + X_{s,1}^{(0)} - X_{s,2}^{(0)} + \sqrt{(X_{\Sigma,1} - X_{\Sigma,2} - X_{s,1}^{(0)} + X_{s,2}^{(0)})^2 + 4X_{\Sigma,1}X_{\Sigma,2}}}, \tag{9}$$

$$X_{s,2} = X_{s,2}^{(0)} \left(1 - X_{s,1}/X_{s,1}^{(0)}\right), \tag{10}$$

where $X_{s,j}^{(0)} \equiv P/K_{H,j}$ is a solubility of a one-component gas. The solution (9), (10) makes physical sense when condition (4) is satisfied; under this condition, equations (9), (10) allow calculating the local equilibrium state for given $X_{\Sigma,1}$ и $X_{\Sigma,2}$.

2.1.2. Temperature and pressure fields

Geological systems are usually much more homogeneous in the horizontal directions than in the vertical. Therefore, we limit our consideration to the one-dimensional case, assuming that the porous medium and the forming structures are homogeneous in the horizontal directions. We assume that the z -axis is directed downward, and its origin is at the surface of the medium.

Let us analyze the propagation of a temperature wave in a porous medium. We will consider harmonic oscillations of the surface temperature $T = T_0 + \Theta_0 \cos \omega t$, where T_0 is the average temperature, Θ_0 is the oscillation amplitude, ω is the cyclic frequency of temperature oscillations. Thus, for example, annual fluctuations in surface temperature deviate only slightly from the harmonic approximation (see, for example, [20]). Heat diffusion equation $\partial T / \partial t = \chi \Delta T$ with no-heat-flux condition deep under the surface (at infinity) and imposed surface temperature yields

$$T(z, t) = T_0 + \Theta_0 e^{-kz} \cos(\omega t - kz), \quad k = \sqrt{\omega / (2\chi)}, \quad (11)$$

where χ is the heat diffusivity and z is the distance from the surface of the porous medium. The pressure field is assumed to be hydrostatic:

$$P = P_0 + \rho g z, \quad (12)$$

where P_0 is the atmospheric pressure, ρ is the density of the liquid, and g is the gravity acceleration.

2.1.3. Diffusion transport equations

Since the insoluble phase cannot move in the pores of the medium, the mass is transferred exclusively by molecular diffusion and is described by the equations

$$\frac{\partial X_{\Sigma, j}}{\partial t} = \frac{\partial}{\partial z} \left(D_j \frac{\partial}{\partial z} X_{s, j} \right), \quad (13)$$

where D_j is the effective coefficient of molecular diffusion of specie j . Compared to the molecular diffusion coefficients in the bulk of a pure liquid ($D_{\text{mol}, j}$), the effective coefficients are affected by the geometry of the pore network (tortuosity of the pore channels) and the adsorption of diffusion agents on the pore matrix. On the time scales of interest in this paper, adsorption does not lead to anomalous diffusion; it only changes the effective rate of normal diffusion [21]. Although the importance of the thermal diffusion effect on geological time scales has been shown for gases [4] and methane hydrates [8, 9], it can be neglected when studying diffusion transport in the system under consideration [5]. Concentrations of dissolved substances are defined by equations (9), (10), if condition (4) is satisfied (when the gas phase is formed). Otherwise, it is equal to total molar fraction $X_{\Sigma, j}$, in this case, $X_{b, j} = 0$.

Equation (13) is accurate if the macroscopic porosity is spatially uniform and the undissolved phase occupies a negligible part of the pore volume, which is true for porous media.

At the upper boundary of the medium there is contact with the atmosphere. This means that $Y_j = Y_{j0}$, where Y_{j0} is the molar fraction of the component in the atmosphere, and, therefore,

$$X_{s, j}(z = 0, t) = \frac{Y_{j0} P_0}{K_{H, j}(T(z = 0, t))}. \quad (14)$$

We assume the absence of both flux and concentration of the undissolved phase deep below the surface:

$$\left. \frac{\partial X_{s,j}}{\partial z} \right|_{z=+\infty} = 0, \tag{15}$$

$$X_{b,j}(z = +\infty) = 0.$$

Note that two boundary conditions are required for $z \rightarrow +\infty$. However, due to the specifics of the problem for $z = 0$, one boundary condition (14) is sufficient. Indeed, since $X_{s,j}(z = 0)$ cannot be less than the solubility, the value of $X_{b,j}$ at the point $z = 0$ does not affect the evolution of the distribution of the dissolved phase, so the condition for it is redundant.

In the general case, all material characteristics of liquids and solutions are functions of temperature and pressure. However, the possible relative changes in the absolute temperature are quite small. Therefore, we can neglect fluctuations in the values of the parameters that are polynomially related to temperature, and consider the non-stationarity for only the parameters that depend exponentially on temperature. These parameters depend on the Henry constant (2) and the molecular diffusion coefficient D_j . The only parameter sensitive to pressure is the solubility of the gas (see equation (3)).

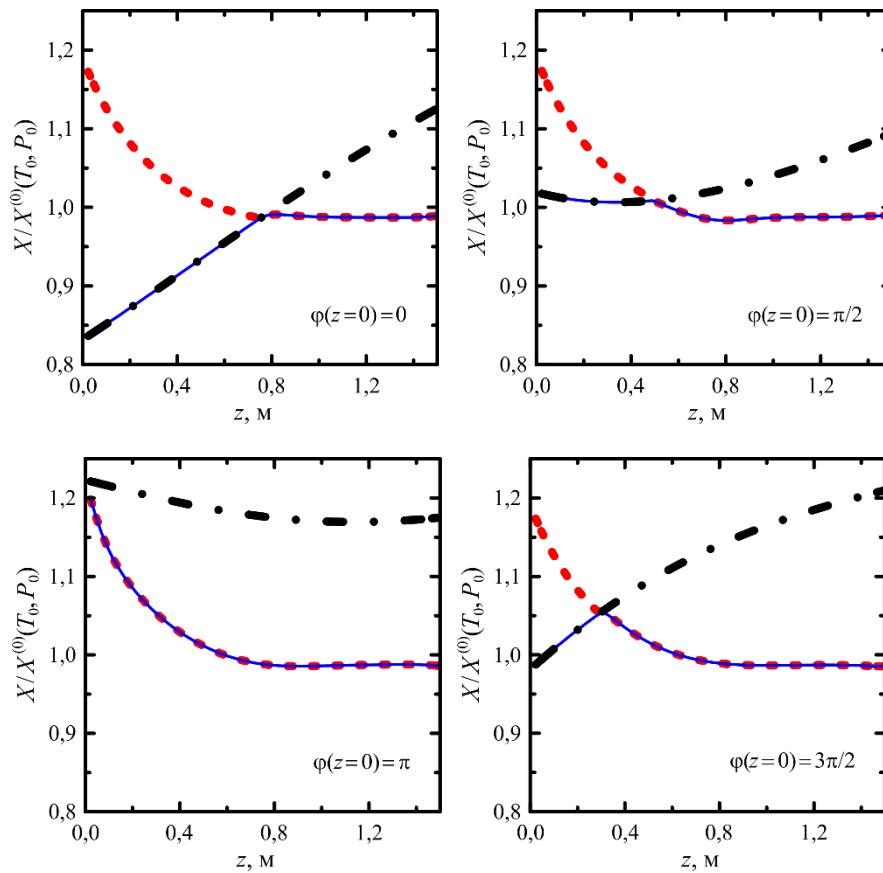


Fig. 1. Profiles of the oscillating solubility of a single-component gas (nitrogen) $X^{(0)}$ formed during the passage of an annual temperature wave in flooded soil at $T_0 = 300$ K, $\Theta_0 = 15$ K at different times (dash-dotted lines): summer $\varphi(z = 0) = 0$, autumn $\varphi(z = 0) = \pi/2$, winter $\varphi(z = 0) = \pi$, spring $\varphi(z = 0) = 3\pi/2$; the solid line is the molar concentration of the solution; dotted line is the net molar fraction of nitrogen in pores X_Σ .

Let us use the following dependence of molecular diffusion on temperature [22];

$$D_{mol,j}(T) = \frac{k_B T}{2\pi\mu R_{d,j}} \frac{\mu + \nu_j}{2\mu + 3\nu_j}, \tag{16}$$

where μ is the dynamic viscosity of the solvent, $R_{d,j}$ is the effective radius of the solute molecules with the coefficient of sliding friction β_j , $\nu_j = R_{d,j}\beta_j/3$ ((equation (16) with the values of the effective radius R_d and parameter ν of the solute molecules given in the table corresponds to the experimental data from [17–19]). The dependence of dynamic viscosity on temperature can be described by the modified Frenkel formula [23]

$$\mu(T) = \mu_0 \exp \frac{a}{T + \tau}. \quad (17)$$

For water, the parameter $\mu_0 = 2,42 \cdot 10^{-5}$ Pa·s, $a = W/k_B = 570$ K (W is the activation energy) and $\tau = -140$ K. For determining the effective diffusion coefficient D_j , we assume that its relative change is related to temperature in the same way as $D_{mol,j}$. The parameter values for aqueous solutions of typical gases are given in the table.

2.2. Numerical simulation

For the numerical simulation, the spatial coordinate was discretized so that the zone of penetration of the undissolved phase L had at least 200 nodes. Simulations demonstrated that fluctuations in the concentration fields of the solution components weakly penetrate beyond this zone, and it is sufficient to set the condition for the absence of a diffusion flux at a double depth as a condition at infinity. At the current time step for the temperature field (11), the fields of Henry's constants (2) were calculated for each of the mixture components. Fields $X_{s,1}$ and $X_{s,2}$ on the surface $z=0$ were set equal to the solubility of the corresponding component at the current time according to (3). In the remaining nodes, the presence of the undissolved phase (4) was checked for the current fields $X_{\Sigma,1}$ and $X_{\Sigma,2}$. If the undissolved phase was missing, the equalities $X_{s,1} = X_{\Sigma,1}$ and $X_{s,2} = X_{\Sigma,2}$ took place. Otherwise, the concentration $X_{s,1}$ and $X_{s,2}$ were calculated by equations (9) and (10). Then, using the difference scheme of equation (9), the fields $X_{\Sigma,1}$ and $X_{\Sigma,2}$ were calculated for the next time step from the current fields $X_{s,1}$ and $X_{s,2}$.

At the first stage, to illustrate the mechanisms of the nonstationary behavior of the system, let us discuss the results of numerical simulation for a single-component atmosphere consisting exclusively of nitrogen. The simulation shows that for any initial state, after the completion of the transition process, the porous medium passes into a single stable time-periodic mode, shown in Figure 1.

The linear increase in solubility with depth (created by the hydrostatic pressure gradient) is modulated by the temperature wave (11). The oscillating profiles of solubility (1), (2) for the temperature wave (11) and pressure (12) are plotted in Fig. 1. The oscillations of the solubility profile create an almost frozen mole fraction $X_{\Sigma}(z)$ profile over time. The molar fraction of the substance in the bubble phase $X_b(z)$ is equal to the difference between the profiles $X_{\Sigma}(z)$ and $X_s(z)$. The mole fraction profile $X_{\Sigma}(z)$ almost reaches its maximum solubility (at minimum temperature in winter) near the surface ($z=0$); here the bubbly fraction exists for almost the entire year, with the exception of the short coldest period. Moreover, $X_{\Sigma}(z)$ monotonically decreases from the depth, where the bubble phase is present, to the depth, where the bubble phase never appears. Further, $X_{\Sigma}(z) = X_s(z)$ is almost homogeneous and only slightly changes throughout the year. The irregularity of the profile $X_{\Sigma}(z)$ in this zone decreases rapidly with depth. The asymptotic value X_{∞} is close to the average annual gas solubility on the surface.

The mole fraction profile is almost constant throughout the year, since the molecular diffusion is 3 orders of magnitude smaller than the thermal diffusivity, which means that the diffusion redistribution of mass is a slow process compared to the rapid temperature (and hence solubility) oscillations. This well-defined division of time scales allows developing an analytical theory of the process, describing the mechanisms of formation of the bubble horizon. Numerical simulation results also become clearer in the context of this theory.

In the case of a two-component atmosphere, the system behavior becomes more complicated since the solubility of the components depends on temperature in different ways and reacts differently to a temperature wave, and the substances themselves diffuse at different rates. One of the main manifestations of this complication is the formation of a diffusion boundary layer in a thin near-surface layer of a porous medium,

which can be seen in Fig. 2. Beyond this boundary layer, the behavior of a two-component medium is similar to that of a one-component medium with some effective parameters. In this case, the diffusion boundary layer introduces nonobvious boundary conditions for this effective single-component medium. In numerical simulations we took into account higher thermal diffusivity of a water-saturated porous medium compared to water and a decrease in effective diffusion due to the complex geometry of pore channels and blockage of some of them; it was assumed that $D_{eff,j}/\chi_{eff} = 0,01D_{mol,j}/\chi$. The results are presented in Fig. 2.

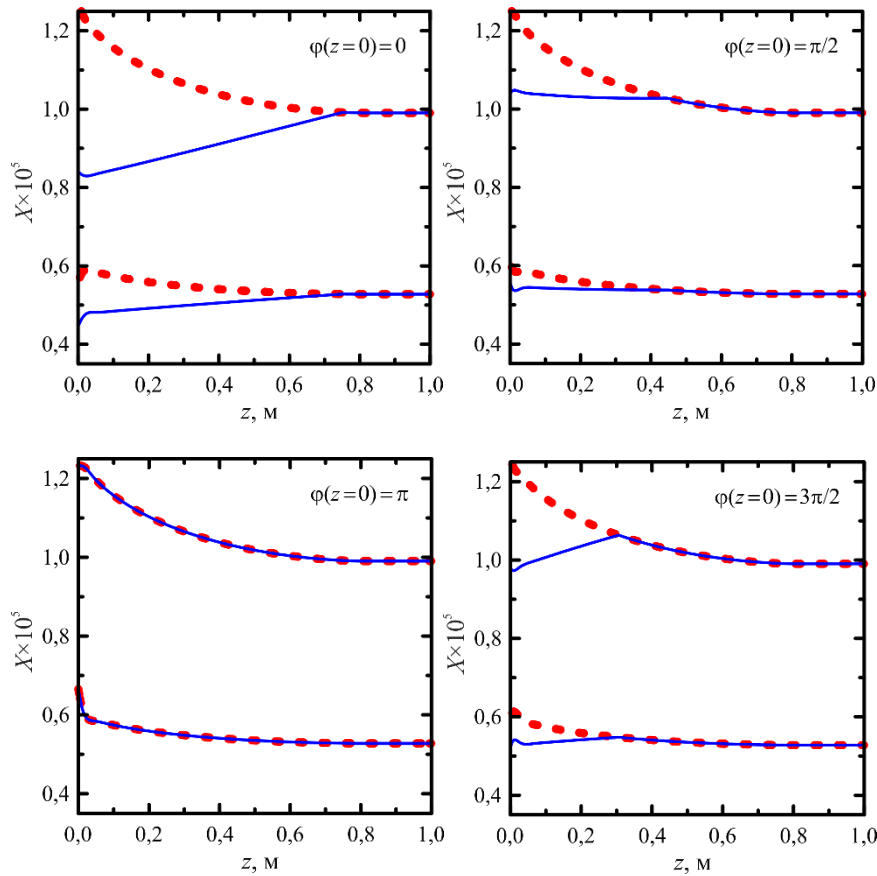


Fig. 2. Profiles of the molar concentration of a two-component gas (a mixture of nitrogen and oxygen) $X_{s,1}$ and $X_{s,2}$ are plotted with the solid lines (the upper one corresponds to nitrogen, the lower one corresponds to oxygen) at $T_0 = 300$ K, $\Theta_0 = 15$ K at different times: summer $\varphi(z=0) = 0$, autumn $\varphi(z=0) = \pi/2$, winter $\varphi(z=0) = \pi$, spring $\varphi(z=0) = 3\pi/2$; the net molar fraction of nitrogen $X_{s,1}$ and oxygen $X_{s,2}$ in pores are plotted with the dotted lines.

3. Analytical theory

To develop an analytical theory, we will assume that temperature fluctuations are small. It is more convenient to start with the basic physical equations and use the smallness of some quantities in the derivation process than to take equations (9), (10) as a basis, and simplify them for the case of small oscillations.

Let us consider two-component gas bubbles in a liquid under a hydrostatic pressure gradient and nonisothermal conditions. The locally equilibrium partial pressure P_j in the gas phase, which is in contact with a solution of a specie j at its molar concentration $X_{s,j}$, is

$$P_j = K_{H,j}(T)X_{s,j}, \tag{18}$$

where $K_{H,j}$ is the Henry's constant for the specie j . For the oscillating temperature $T = T_0 + \Theta_0 \cos \omega t$ at the interface between bottom sediments and the atmosphere, the temperature field inside the sediments is

$$T(z, t) = T_0 + \Theta(z, t) = T_0 + \Theta_0 e^{-kz} \cos(\omega t - kz) = T_0 + \Theta_0 e^{-kz} \cos \varphi, \tag{19}$$

where $\varphi = \omega t - kz$ is the phase of temperature oscillation, $k = \sqrt{\omega/(2\chi)}$, z is the distance from the surface of porous medium, χ is the heat diffusivity. Thus, locally equilibrium concentrations of solutes $X_{s,j}$ in the presence of bubbles of a two-component gas obey the equation

$$K_{H,1} X_{s,1} + K_{H,2} X_{s,2} = P_0 (1 + bz), \tag{20}$$

where P_0 is the atmospheric pressure, $b = \rho_l g / P_0$, ρ_l is the liquid density, g is the gravity acceleration. Let us introduce the notation

$$K_j = \frac{K_{H,j}}{P_0}$$

and linearize the dependence of Henry's constants on temperature:

$$K_j = K_{j0} \left(1 + a_j \Theta + O\left((a_j \Theta)^2 \right) \right), \tag{21}$$

where $K_{j0} = K_j(T_0)$, $a_j = \frac{1}{K_j} \left(\frac{\partial K_j}{\partial T} \right)_{T_0}$.

The ratio of the number of molecules in the gas phase is $X_{b,1}/X_{b,2} = P_1/P_2$. In accordance with equation (18), one can get

$$\frac{X_{\Sigma,1} - X_{s,1}}{X_{\Sigma,2} - X_{s,2}} = \frac{K_1 X_{s,1}}{K_2 X_{s,2}}.$$

When the relative changes in solubility are small, the left side of the last equality is the ratio of small quantities and the right side is the ratio of non-small quantities, the values of which are slightly perturbed by the change in K_j and pressure. Therefore, we can approximately assume the constancy of this ratio, which means the constancy of the composition of the gas phase, as was observed in the numerical simulation;

$$\frac{X_{\Sigma,1} - X_{s,1}}{X_{\Sigma,2} - X_{s,2}} \approx \frac{Y_{10}}{Y_{20}}, \tag{22}$$

where $Y_{j0} = K_{j0} X_{s,j0}$ is the molar fraction of specie j in atmosphere. One can notice, that

$$Y_{10} + Y_{20} = 1.$$

Let us consider the deviation of the mass distribution of gas in liquid in pores from the state without temperature oscillations;

$$X_{\Sigma,j} \Big|_{\Theta_0=0} = X_{s,j} \Big|_{\Theta_0=0} = X_{s,j0} = \frac{Y_{j0}}{K_{j0}}.$$

Then,

$$\begin{aligned} X_{\Sigma,j} &= X_{s,j0} + X_{\Sigma,j}^{\sim}, \\ X_{s,j} &= X_{s,j0} + X_{s,j}^{\sim}. \end{aligned}$$

In terms of deviations $X_{\Sigma,j}^{\sim}$ and $X_{s,j}^{\sim}$, equation (20) to leading order reads

$$K_{10}X_{s,1}^{\sim} + K_{20}X_{s,2}^{\sim} = bz - \Theta \sum_j a_j Y_{j0}, \tag{23}$$

and equation (22) yields

$$Y_{20}X_{s,1}^{\sim} - Y_{10}X_{s,2}^{\sim} = Y_{20}X_{\Sigma,1}^{\sim} - Y_{10}X_{\Sigma,2}^{\sim}. \tag{24}$$

Equations (23), (24) form a self-consistent system for $X_{s,j}^{\sim}$ as a function of Θ and $X_{\Sigma,j}^{\sim}$. Note that equations (23), (24) are valid for the zone of sediments, where $X_{\Sigma,j}$ is sufficient for the formation of the gas phase, i.e., in accordance with equation (23), $\Theta > \Theta(\varphi_*)$. The value of $X_{\Sigma,j}$ is determined from the following equation;

$$K_{10}X_{\Sigma,1}^{\sim} + K_{20}X_{\Sigma,2}^{\sim} = bz - \Theta(\varphi_*) \sum_j a_j Y_{j0}. \tag{25}$$

For $\Theta < \Theta(\varphi_*)$, all guest gas molecules are dissolved and $X_{s,j}^{\sim} = X_{\Sigma,j}^{\sim}$.

The transport of guest molecules is carried out through the liquid phase due to the molecular diffusion of the solution. Due to the smallness of the ratio of the coefficients of molecular diffusion and thermal diffusivity in liquids, the profiles of the concentrations $X_{\Sigma,j}$ are almost “frozen” on the time scale of one period of temperature oscillation. Therefore, it suffices to calculate the molecular diffusion flux averaged over a period.

In the zone of a porous medium, where bubbles appear on a certain part of the oscillation period, one obtains

$$\langle J_j \rangle = \frac{1}{t_p} \int_{t_1}^{t_2} \left(-D_j \frac{\partial X_{s,j}^{\sim}}{\partial z} \right) dt + \frac{1}{t_p} \int_{t_2}^{t_1+t_p} \left(-D_j \frac{\partial X_{\Sigma,j}^{\sim}}{\partial z} \right) dt. \tag{26}$$

Here $t_p = 2\pi/\omega$ is the oscillation period; $t_1 < t_2$ are the time points between which the local temperature is sufficiently high, $\Theta > \Theta(\varphi_*)$, so that not all of the guest gas molecules can be dissolved and the solution flow is controlled by the concentration gradient of the dissolved substance $dX_{s,j}^{\sim}/dz$, described by the equation system (23), (24). For the rest of the period, the equality $X_{s,j}^{\sim} = X_{\Sigma,j}^{\sim}$ is true, and the solute flux is controlled by concentration gradient of guest molecules. Equation (26) can be recast in terms of the phase of temperature fluctuations:

$$\langle J_j \rangle = \frac{1}{2\pi} \int_{-\varphi_*}^{\varphi_*} \left(-D_j \frac{\partial X_{s,j}^{\sim}}{\partial z} \right) d\varphi + \frac{1}{2\pi} \int_{\varphi_*}^{\varphi_*+2\pi} \left(-D_j \frac{\partial X_{\Sigma,j}^{\sim}}{\partial z} \right) d\varphi. \tag{27}$$

4. Diffusion boundary layer

For one-component gas, the assumption of “frozen” profiles $X_{\Sigma,j}$ is accurate [6], since the solubility profile is strictly determined by temperature and pressure, and diffusion transfer along the solubility gradient is slow. A diffusion boundary layer is not formed near the surface. The case of a two-component gas turns out to be significantly different, because changing the composition of the gas affects the solubility, and the concentration profiles of the dissolved substances depend not only on the temperature and pressure fields. Indeed, Fig. 2 shows a diffusion boundary layer with short-wave oscillations near the surface, which are never observed in a one-component gas. This boundary layer must be taken into account, since inside it the profiles $X_{\Sigma,j}$ are actually “not frozen”, although outside it they can be considered “frozen”. The diffusion boundary layer can affect the effective boundary conditions of the concentration fields in the zones of “frozen” profiles.

Since the diffusion boundary layer is localized near the surface on an incomparably smaller scale than the scale of the temperature wave, we can assume the spatial homogeneity of the temperature field, $\Theta(z, t) = \Theta_0 \cos \omega t$, and neglect the hydrostatic pressure gradient.

Diffusion transport is carried out through the solution, while the diffusion coefficients are spatially homogeneous (for a uniform temperature field);

$$\frac{\partial}{\partial t} X_{\Sigma, j}^{\sim} = D_j(\Theta) \frac{\partial^2}{\partial z^2} X_{s, j}^{\sim}. \tag{28}$$

Numerical simulation shows that in the diffusion boundary layer with a spatially homogeneous solubility field oscillating in time, the solute is undersaturated (the bubble phase disappears) only during a short part of the oscillatory cycle, and this part tends to zero when the ratio D_j/χ tends to zero. Therefore, we can approximately assume that the bubble phase is always present, and the concentration fields $X_{s, j}^{\sim}$ obey equations (23) and (24).

In the absence of a hydrostatic pressure gradient, equations (23) has the form

$$K_{10} X_{s, 1}^{\sim} + K_{20} X_{s, 2}^{\sim} = -a_{12} \Theta, \tag{29}$$

where

$$a_{12} = Y_{10} a_1 + Y_{20} a_2. \tag{30}$$

Equations (29) и (24) yield

$$K_{12} X_{s, 1}^{\sim} = -Y_{10} a_{12} \Theta + K_{20} (Y_{20} X_{\Sigma, 1}^{\sim} - Y_{10} X_{\Sigma, 2}^{\sim}), \tag{31}$$

$$K_{12} X_{s, 2}^{\sim} = -Y_{20} a_{12} \Theta - K_{10} (Y_{20} X_{\Sigma, 1}^{\sim} - Y_{10} X_{\Sigma, 2}^{\sim}), \tag{32}$$

where

$$K_{12} = Y_{10} K_{10} + Y_{20} K_{20}. \tag{33}$$

Substituting (32) and (33) into equation (28) for $j = 1, 2$ yields

$$\frac{\partial}{\partial t} X_{\Sigma, 1}^{\sim} = \frac{D_1 K_{20}}{K_{12}} \frac{\partial^2}{\partial z^2} (Y_{20} X_{\Sigma, 1}^{\sim} - Y_{10} X_{\Sigma, 2}^{\sim}),$$

$$\frac{\partial}{\partial t} X_{\Sigma, 2}^{\sim} = -\frac{D_2 K_{10}}{K_{12}} \frac{\partial^2}{\partial z^2} (Y_{20} X_{\Sigma, 1}^{\sim} - Y_{10} X_{\Sigma, 2}^{\sim}).$$

The latter equation system means, that the field

$$X_{\Sigma, b.l.}^{\sim}(z) \equiv D_2 K_{10} X_{\Sigma, 1}^{\sim} + D_1 K_{20} X_{\Sigma, 2}^{\sim} \tag{34}$$

remains constant over time and

$$\frac{\partial}{\partial t} X_{\Sigma, res}^{\sim} = D_{12} \frac{\partial^2}{\partial z^2} X_{\Sigma, res}^{\sim}, \tag{35}$$

where

$$X_{\Sigma, res}^{\sim} \equiv Y_{20} X_{\Sigma, 1}^{\sim} - Y_{10} X_{\Sigma, 2}^{\sim}, \tag{36}$$

$$D_{12} \equiv \frac{D_2 K_{10} Y_{10} + D_1 K_{20} Y_{20}}{K_{12}}.$$

The original variables can be expressed from $X_{\Sigma, b.l.}^{\sim}$ and $X_{\Sigma, res}^{\sim}$ as follows;

$$X_{\Sigma, 1}^{\sim} = \frac{Y_{10} X_{\Sigma, b.l.}^{\sim} + D_1 K_{20} X_{\Sigma, res}^{\sim}}{D_1 K_{20} Y_{20} + D_2 K_{10} Y_{10}},$$

$$X_{\Sigma, 2}^{\sim} = \frac{Y_{20} X_{\Sigma, b.l.}^{\sim} - D_2 K_{10} X_{\Sigma, res}^{\sim}}{D_1 K_{20} Y_{20} + D_2 K_{10} Y_{10}}.$$

The solution of equation (35) is a wave that decays exponentially with z (which remains accurate for time-dependent $D_{12}(\Theta)$). Therefore, outside the diffusion boundary layer $X_{\Sigma, res}^{\sim} = 0$, and the fields $X_{\Sigma, j}^{\sim}$ are determined by the fields $X_{\Sigma, b.l.}^{\sim}$. For the surface, $X_{\Sigma, j}^{\sim}(0) = Y_{j0} a_j \Theta_0 / K_{j0}$ (which corresponds to the maximum value of the solution concentration for the period). Thus,

$$X_{\Sigma, b.l.}^{\sim} = D_2 Y_{10} a_1 \Theta_0 + D_1 Y_{20} a_2 \Theta_0$$

and for the surface, immediately behind the diffusion boundary layer,

$$X_{\Sigma, j}^{\sim} = \frac{Y_{j0} (D_2 Y_{10} a_1 \Theta_0 + D_1 Y_{20} a_2 \Theta_0)}{D_2 K_{10} Y_{10} + D_1 K_{20} Y_{20}}. \tag{37}$$

Equation (37) provides effective boundary conditions at $z = 0$ for solutions with a “frozen” profile outside the diffusion boundary layer.

5. Transport processes beyond diffusion boundary layer

5.1. The case of small solubility oscillation amplitude and bubbly horizon penetration depth

For a better understanding of the system behavior, it is convenient to consider the simplest case that admits an analytical solution. To do this, we assume not only the smallness of fluctuations in solubility and the molecular diffusion coefficient, but also take into account the smallness of the penetration depth of the bubble horizon at a small amplitude of temperature fluctuations, $e^{-kz} \approx 1$.

To the leading order, equation (27) for $j = 1$ yields

$$\langle J_1 \rangle = -D_{10} \frac{1}{2\pi} \int_{-\varphi_*}^{\varphi_*} \frac{\partial X_{s,1}^{\sim}}{\partial z} d\varphi - D_{10} \left(1 - \frac{\varphi_*}{\pi} \right) \frac{\partial X_{\Sigma, 1}^{\sim}}{\partial z}, \tag{38}$$

where $D_{j0} = D_j(T_0)$. Equations (23), (24) yield

$$K_{12} X_{s,1}^{\sim} = b Y_{10} z - Y_{10} a_{12} \Theta + K_{20} (Y_{20} X_{\Sigma, 1}^{\sim} - Y_{10} X_{\Sigma, 2}^{\sim}). \tag{39}$$

Since $\langle J_1 \rangle = 0$ for a stable distribution of the dissolved substance, one can get from equations (38) and (39)

$$0 = -D_{10} \left[\frac{\varphi_*}{\pi K_{12}} \left(bY_{10} + K_{20} \left(Y_{20} \frac{dX_{\Sigma,1}^-}{dz} - Y_{10} \frac{dX_{\Sigma,2}^-}{dz} \right) \right) + \frac{ka_{12}\Theta_0}{\pi} \frac{Y_{10}}{K_{12}} \sin \varphi_* + \left(1 - \frac{\varphi_*}{\pi} \right) \frac{dX_{\Sigma,1}^-}{dz} \right]. \quad (40)$$

Simplifying the latter equation and performing similar calculations for substance 2 yield

$$Y_{10} \left[\frac{\varphi_*}{\pi} \left(b - K_{10} \frac{dX_{\Sigma,1}^-}{dz} - K_{20} \frac{dX_{\Sigma,2}^-}{dz} \right) + \frac{ka_{12}\Theta_0}{\pi} \sin \varphi_* \right] + K_{12} \frac{dX_{\Sigma,1}^-}{dz} = 0, \quad (41)$$

$$Y_{20} \left[\frac{\varphi_*}{\pi} \left(b - K_{10} \frac{dX_{\Sigma,1}^-}{dz} - K_{20} \frac{dX_{\Sigma,2}^-}{dz} \right) + \frac{ka_{12}\Theta_0}{\pi} \sin \varphi_* \right] + K_{12} \frac{dX_{\Sigma,2}^-}{dz} = 0. \quad (42)$$

5.1.1. Single-component gas

In the case of a single-component gas ($Y_{20} = 0$ and $X_{\Sigma,2}^- = 0$), system (41), (42) can be simplified to

$$\varphi_* b + ka_1\Theta_0 \sin \varphi_* + K_{10} (\pi - \varphi_*) \frac{dX_{\Sigma,1}^-}{dz} = 0, \quad (43)$$

and equation (25) for φ_* turns into

$$K_{10} X_{\Sigma,1}^- = bz - a_1\Theta_0 \cos \varphi_*. \quad (44)$$

Applying relation (44), one can recast equation (43) in terms of φ_* ;

$$\pi b + ka_1\Theta_0 \sin \varphi_* + (\pi - \varphi_*) a_1\Theta_0 \sin \varphi_* \frac{d\varphi_*}{dz} = 0.$$

Let us introduce new dimensionless variables $\xi = \frac{bz}{a_{12}\Theta_0}$, $\varkappa = \frac{ka_{12}\Theta_0}{b}$ (in this case $a_{12} = a_1$). The dimensionless equation for φ_* reads

$$\pi + \varkappa \sin \varphi_* + (\pi - \varphi_*) \sin \varphi_* \frac{d\varphi_*}{d\xi} = 0. \quad (45)$$

The characteristic values of the dimensionless coordinate ξ are of the order of 1, so the assumption $kz = \varkappa\xi \ll 1$ requires $\xi \ll 1$. Therefore, the second term in equation (44) can be neglected. Thus,

$$\pi + (\pi - \varphi_*) \sin \varphi_* \frac{d\varphi_*}{d\xi} = 0, \quad (46)$$

which is identical to equation (19) in [6] and can be integrated with the initial value $\varphi_*(\xi = 0) = \pi$;

$$(\pi - \varphi_*) \cos \varphi_* + \sin \varphi_* = \pi\xi. \quad (47)$$

Equation (47) provides an implicit dependence of φ_* on the coordinate ξ . The field $\varphi_*(\xi)$ decreases monotonically with depth ξ from $\varphi_*(0) = \pi$ to $\varphi_*(1) = 0$. The penetration depth of the bubble horizon is $\xi_b = 1$. With a known field $\varphi_*(bz/(a_1\Theta_0))$, one can use equation (44) to find $X_{\Sigma,1}^-(z)$.

Below the penetration depth of the bubble horizon $\xi_b = 1$, the solute concentration is spatially uniform and constant in time. To the leading order,

$$X_{\Sigma,1}^{\sim}(\infty)\Big|_{Y_{20}=0} = 0. \tag{48}$$

5.1.2. Two-component gas

As was shown for a single-component gas, the consistency of the approximation $kz \ll 1$ assumes that the term $ka_{12}\Theta_0 \sin \varphi_*$ in equations (41) and (42) is neglected. The sum of products of equation (23) by K_{10} and equation (24) by K_{20} yields

$$\frac{\varphi_*}{\pi} \left(b - \frac{dZ}{dz} \right) + \frac{dZ}{dz} = 0, \tag{49}$$

where

$$Z = K_{10}X_{\Sigma,1}^{\sim} + K_{20}X_{\Sigma,2}^{\sim}. \tag{50}$$

Equation (25) in terms of Z reads

$$Z = bz - a_{12}\Theta_0 \cos \varphi_*. \tag{51}$$

Substituting Z from equation (51) into equation (49), one obtain an equation identical to (46) in terms of $\varphi_*(\xi)$. However, it should be integrated with boundary conditions that take into account the diffusion boundary layer (37);

$$Z(0) = K_{12} \frac{D_2 Y_{10} a_1 \Theta_0 + D_1 Y_{20} a_2 \Theta_0}{D_2 K_{10} Y_{10} + D_1 K_{20} Y_{20}}.$$

In this case, $\varphi_*(0)$ does not equal to π as in the case of a single-component gas. However, according to equation (51),

$$\cos \varphi_*(0) = - \frac{Y_{10} K_{10} + Y_{20} K_{20}}{Y_{10} a_1 + Y_{20} a_2} \frac{D_2 Y_{10} a_1 + D_1 Y_{20} a_2}{D_2 K_{10} Y_{10} + D_1 K_{20} Y_{20}}. \tag{52}$$

Then, instead of equation (47), one obtains

$$(\pi - \varphi_*) \cos \varphi_* + \sin \varphi_* = \pi (\xi + 1 - \xi_b), \tag{53}$$

where the penetration depth of the bubble horizon

$$\xi_b = 1 - \frac{[\pi - \varphi_*(0)] \cos \varphi_*(0) + \sin \varphi_*(0)}{\pi}.$$

is decreased compared to the case of a single-component gas.

The difference between the products of equation (23) by Y_{20} and equation (24) by Y_{10} is

$$\frac{d}{dz} X_{\Sigma,res}^{\sim} = 0,$$

where $X_{\Sigma, res}^{\sim}$ is determined from equation (36). Taking into account the boundary condition (37) yields $X_{\Sigma, res}^{\sim} = 0$.

The distribution of components can be calculated from the expressions for Z and $X_{\Sigma, res}^{\sim}$;

$$X_{\Sigma, 1}^{\sim} = \frac{Y_{10}Z + K_{20}X_{\Sigma, res}^{\sim}}{K_{12}} = \frac{Y_{10}}{K_{12}}(bz - a_{12}\Theta_0 \cos \varphi_*), \tag{54}$$

$$X_{\Sigma, 2}^{\sim} = \frac{Y_{20}Z - K_{10}X_{\Sigma, res}^{\sim}}{K_{12}} = \frac{Y_{20}}{K_{12}}(bz - a_{12}\Theta_0 \cos \varphi_*). \tag{55}$$

Below the penetration depth of the bubble horizon ξ_b (where $\varphi_* = 0$) the concentration of the solution is spatially homogeneous and constant in time. To the leading order,

$$X_{\Sigma, 1\infty}^{\sim} = X_{\Sigma, 2\infty}^{\sim} = 0,$$

which means that the composition of the solution does not change compared to the case of no temperature oscillation.

To summarize this section, we note that in terms of φ_* the case of a two-component atmosphere is similar to the case of a single-component atmosphere with the effective parameter a_{12} instead of a_j and K_{12} instead of K_{j0} . However, the diffusion boundary layer noticeably reduces the uppermost part of the bubble horizon. Indeed, for a single-component gas $\varphi_*(0) = \pi$, and for a two-component gas $\varphi_*(0)$ is determined from equation (52), i.e., the profile for a two-component atmosphere is the profile for a one-component atmosphere shifted towards the surface.

It is important to note that the developed analytical theory is an approximation, not a strict limiting case. The analytic theory requires smallness of Θ_0 . Meanwhile, at small values of Θ_0 , the penetration depth of the bubble zone is small (one can see from the definition of ξ that the penetration depth is a linear function of Θ_0) and can become comparable with the thickness of the diffusion boundary layer:

$$\delta_{diff} = \sqrt{2D_{12}/\omega}.$$

In this case, the approximation of “frozen” profiles $X_{\Sigma, j}(z)$ is not applicable. Thus, the “frozen” profile approximation is not compatible with the limit $\Theta_0 \rightarrow 0$. Nevertheless, for moderately small Θ_0 , both approximations can be quite accurate.

5.2. Moderate penetration depth of bubble horizon

The theory formulated for the case of a shallow penetration depth of the bubble layer makes it possible to obtain an analytical solution, which significantly improves the understanding of the system dynamics, and to evaluate its characteristic feature such as the relationship between the penetration depth and the amplitude of temperature oscillation Θ_0 . Taking the theoretical description of this medium as a basis, we can proceed to the problem constructing a theory for a moderate penetration depth, when kz (or $\mathcal{R}\xi$) is not small in the bubble zone.

In this case, the calculation of the average diffusion fluxes (27) requires taking into account the dependence of diffusion coefficients on the temperature;

$$D_j(T) = D_{j0} \left(1 + \gamma_j \Theta + O\left((\gamma_j \Theta)^2 \right) \right). \tag{56}$$

After time-consuming but obvious calculations, one can get an improved version of the system of equations (41), (42);

$$\begin{aligned}
 & Y_{10} \left[\frac{(\varphi_* + \gamma_1 \Theta_0 e^{-kz} \sin \varphi_*)}{\pi} \left(b - \sum_j K_{j0} \frac{dX_{\Sigma,j}^-}{dz} \right) + \right. \\
 & \left. + \frac{ka_{12}}{\pi} \left(\Theta_0 e^{-kz} \sin \varphi_* + \frac{\gamma_1 \Theta_0^2}{2} e^{-2kz} \left(\varphi_* - \frac{1}{2} \sin 2\varphi_* \right) \right) \right] + K_{12} \frac{dX_{\Sigma,2}^-}{dz} = 0, \tag{57}
 \end{aligned}$$

$$\begin{aligned}
 & Y_{20} \left[\frac{(\varphi_* + \gamma_2 \Theta_0 e^{-kz} \sin \varphi_*)}{\pi} \left(b - \sum_j K_{j0} \frac{dX_{\Sigma,j}^-}{dz} \right) + \right. \\
 & \left. + \frac{ka_{12}}{\pi} \left(\Theta_0 e^{-kz} \sin \varphi_* + \frac{\gamma_2 \Theta_0^2}{2} e^{-2kz} \left(\varphi_* - \frac{1}{2} \sin 2\varphi_* \right) \right) \right] + K_{12} \frac{dX_{\Sigma,2}^-}{dz} = 0. \tag{58}
 \end{aligned}$$

The sum of equation (57) multiplied by K_{10} , and equation (58) multiplied by K_{20} , is equal to

$$\frac{(\varphi_* + \gamma_{12} \Theta_0 e^{-kz} \sin \varphi_*)}{\pi} \left(b - \frac{dZ}{dz} \right) + \frac{ka_{12}}{\pi} \left(\Theta_0 e^{-kz} \sin \varphi_* + \frac{\gamma_{12} \Theta_0^2}{2} e^{-2kz} \left(\varphi_* - \frac{1}{2} \sin 2\varphi_* \right) \right) + \frac{dZ}{dz} = 0, \tag{59}$$

where

$$\gamma_{12} = \frac{\gamma_1 Y_{10} K_{10} + \gamma_2 Y_{20} K_{20}}{Y_{10} K_{10} + Y_{20} K_{20}}. \tag{60}$$

Equation (25) for φ_* yields

$$Z = bz - a_{12} \Theta_0 e^{-kz} \cos \varphi_*. \tag{61}$$

Substituting equation (61) into equation (59), one can rewrite the latter one in a dimensionless form for $F = e^{-\varkappa \xi} \cos \varphi_*$ (also bearing in mind that $Z = bz - a_{12} \Theta_0 F$):

$$\frac{d\xi}{dF} = \frac{\pi - \arccos(F e^{\varkappa \xi}) - \gamma_{12} \Theta_0 \sqrt{e^{-2\varkappa \xi} - F^2}}{\pi + \frac{1}{2} \varkappa \gamma_{12} \Theta_0 e^{-2\varkappa \xi} \arccos(F e^{\varkappa \xi}) + \varkappa \left(1 - \frac{1}{2} \gamma_{12} \Theta_0 F \right) \sqrt{e^{-2\varkappa \xi} - F^2}}. \tag{62}$$

Equation (62) can be integrated from the initial conditions $\xi(F = \cos \varphi_*(0)) = 0$ (on the surface) to the point where the $F = e^{-\varkappa \xi}$ (at the bottom of the bubble horizon); $\cos \varphi_*(0)$ is determined from equation (52). Here we intentionally integrate $(d\xi/dF)$ instead of $(dF/d\xi)$, since this allows taking into account the singularities $dF/d\xi = \infty$ on the surface.

Now one can calculate the quantitative indicators of the solution composition. As in the case of shallow penetration, subtracting Eq. (58) multiplied by Y_{10} from Eq. (57) multiplied by Y_{20} yields the differential equation for $X_{\Sigma,res}^- = Y_{20} X_{\Sigma,1}^- - Y_{10} X_{\Sigma,2}^-$:

$$\frac{d}{dz} X_{\Sigma,res}^- = \frac{Y_{10} Y_{20}}{\pi} (\gamma_1 - \gamma_2) a_{12} \Theta_0^2 \left[-e^{-kz} \sin \varphi_* \frac{d}{dz} (e^{-kz} \cos \varphi_*) - \frac{k}{2} e^{-2kz} \left(\varphi_* - \frac{1}{2} \sin 2\varphi_* \right) \right].$$

The latter equation can be recast to a dimensionless form, which is convenient for integration together with Eq. (62):

$$dX_{\Sigma,res}^- = \frac{Y_{10} Y_{20}}{\pi} (\gamma_1 - \gamma_2) a_{12} \Theta_0^2 \left[-\sqrt{e^{-2\varkappa \xi} - F^2} dF - \frac{\varkappa}{2} \left(e^{-2\varkappa \xi} \arccos(e^{\varkappa \xi} F) - F \sqrt{e^{-2\varkappa \xi} - F^2} \right) d\xi \right]. \tag{63}$$

The value of $X_{\Sigma, res}^{\sim}$ on the surface is determined according to the boundary condition (37):

$$X_{\Sigma, res}^{\sim} \Big|_{z=0} = 0, \quad (64)$$

which serves as the initial condition for integrating Eq. (63). For given Z and $X_{\Sigma, res}^{\sim}$, one can get

$$X_{\Sigma, 1}^{\sim} = \frac{Y_{10}Z + K_{20}X_{\Sigma, res}^{\sim}}{K_{12}}, \quad (65)$$

$$X_{\Sigma, 2}^{\sim} = \frac{Y_{20}Z - K_{10}X_{\Sigma, res}^{\sim}}{K_{12}}. \quad (66)$$

Note that the value of $X_{\Sigma, res}^{\sim}$ (equations (63), (64)) has a higher order of smallness in Θ_0 than Z . Thus, it is small for small fluctuations in solubility. Moreover, it is also proportional to the difference in the temperature dependence of the diffusion coefficients $(\gamma_1 - \gamma_2)$. If $\gamma_1 = \gamma_2$, discrepancies in D_{j0} or in the solubility properties of the first and second components cannot lead to a change of $X_{\Sigma, res}^{\sim}$ within the bubble layer. Thus, the composition of the solution under the bubbly horizon in leading order by Θ_0 is as follow:

$$X_{\Sigma, 1\infty}^{\sim} \approx X_{\Sigma, 2\infty}^{\sim} \approx 0.$$

This means that the composition of the solution does not change compared to the case without temperature oscillations.

6. Conclusion

The effect of harmonic surface temperature oscillations on the infiltration of a weakly soluble substance in a liquid-saturated porous medium is considered. These oscillations create a temperature wave that propagates in the porous medium from the surface deep inside and attenuates. The solubility wave associated with the temperature wave leads to a time-dependent alternation of zones of the undissolved phase with the saturated solution and the zones of an undersaturated solution. Due to the smallness of the ratio D/χ ($\sim 10^{-3}$ for typical liquids), diffusion transfer in a porous medium occurs much slower than the temperature (and solubility) changes. As a result, the profile of the net mole fraction of guest molecules in the pores X_{Σ} (“net” means “solute + undissolved phase”) remains almost constant throughout the oscillation period. For gases, the profile almost reaches its maximum solubility for the period near the surface and monotonically decays with depth in the zone where the undissolved phase can be observed (the so-called “bubble horizon”) and remains at a constant level below the bubble horizon. At any depth z , the bubble phase disappears only for a short part of the oscillation period; in the limiting case ($D/\chi \rightarrow 0$), this part of the oscillation period also tends to zero.

The appearance of a near-surface diffusion boundary layer for the case of multicomponent gases is of interest in the described system. This boundary layer does not arise for single-component guest substances, since in the specified thin near-surface zone the concentration profile is the solubility one, which is unambiguously dictated by the temperature field. For single-component guest substances, this boundary layer never appears, since in this thin near-surface zone the concentration profile is the solubility one, which is dictated by the temperature field. For multicomponent gases, the total solubility depends on the relative proportions of the components. If the components diffuse at different rates, the nonstationarity of the concentration on the surface creates an unequal redistribution of the components in the solution and the bubble phase. This oscillating nonstationarity causes the nonstationarity of solubility. Since the mechanism of transport of component molecules is diffusion, the spatial scale of penetration of these solubility fluctuations is determined by the diffusion coefficient. It is appropriate to call the zone of such unsteady behavior the diffusion boundary layer. In the paper it is shown that beyond its limits it is possible to set effective boundary conditions for the gas mixture composition (see equation (37)), and the transport of gases can be considered

as corresponding to the transport of a single-component gas with effective solubility parameters and its temperature dependence (33) and (30).

Previously, a strong nonlinear effect of freezing waves arising from temperature fluctuations was established and theoretically studied if the minimum temperatures fall below the freezing point of the liquid [24]. In porous media with active methane released from sediments, freezing waves can lead to the formation of bubble horizons. In the case of passive media considered in this work (without a source of matter distributed over the volume), the transfer of multicomponent gases should involve a nontrivial interaction between the diffusion boundary layer and freezing waves.

The work was supported by the Ministry of Science and Higher Education of the Russian Federation (theme no. 121112200078-7).

References

1. Donaldson J.H., Istok J.D., Humphrey M.D., O'Reilly K.T., Hawelka C.A., Mohr D.H. Development and testing of a kinetic model for oxygen transport in porous media in the presence of trapped gas. *Groundwater*, 1997, vol. 35, pp. 270-279. <https://doi.org/10.1111/j.1745-6584.1997.tb00084.x>
2. Donaldson J.H., Istok J.D., O'Reilly K.T. Dissolved gas transport in the presence of a trapped gas phase: Experimental evaluation of a two-dimensional kinetic model. *Groundwater*, 1998, vol. 36, pp. 133-142. <https://doi.org/10.1111/J.1745-6584.1998.TB01073.X>
3. Haacke R.R., Westbrook G.K., Riley M.S. Controls on the formation and stability of gas hydrate-related bottom-simulating reflectors (BSRs): A case study from the west Svalbard continental slope. *J. Geophys. Res.: Solid Earth*, 2008, vol. 113, B05104. <https://doi.org/10.1029/2007JB005200>
4. Goldobin D.S., Brilliantov N.V. Diffusive counter dispersion of mass in bubbly media. *Phys. Rev. E*, 2011, vol. 84, 056328. <https://doi.org/10.1103/physreve.84.056328>
5. Krauzin P.V., Goldobin D.S. Effect of temperature wave on diffusive transport of weakly soluble substances in liquid-saturated porous media. *Eur. Phys. J. Plus*, 2014, vol. 129, 221. <https://doi.org/10.1140/epjp/i2014-14221-1>
6. Goldobin D.S., Krauzin P.V. Formation of bubbly horizon in liquid-saturated porous medium by surface temperature oscillation. *Phys. Rev. E*, 2015, vol. 92, 063032. <https://doi.org/10.1103/PhysRevE.92.063032>
7. Davie M.K., Buffett B.A. A numerical model for the formation of gas hydrate below the seafloor. *J. Geophys. Res.: Solid Earth*, 2001, vol. 106, pp. 497-514. <http://dx.doi.org/10.1029/2000JB900363>
8. Goldobin D.S. Non-Fickian diffusion affects the relation between the salinity and hydrate capacity profiles in marine sediments. *Compt. Rendus Mec.*, 2013, vol. 341, pp. 386-392. <http://dx.doi.org/10.1016/j.crme.2013.01.014>
9. Goldobin D.S., Brilliantov N.V., Levesley J., Lovell M.A., Rochelle C.A., Jackson P.D., Haywood A.M., Hunter S.J., Rees J.G. Non-Fickian diffusion and the accumulation of methane bubbles in deep-water sediments. *Eur. Phys. J. E*, 2014, vol. 37, 45. <http://dx.doi.org/10.1140/epje/i2014-14045-x>
10. Petit J.R., Jouzel J., Raynaud D., Barkov N.I., Barnola J.-M., Basile I., Bender M., Chappellaz J., Davis M., Delaygue G., Delmotte M., Kotlyakov V.M., Legrand M., Lipenkov V.Y., Lorius C., Pépin L., Ritz C., Saltzman E., Stievenard M. Climate and atmospheric history of the past 420,000 years from the Vostok ice core, Antarctica. *Nature*, 1999, vol. 399, pp. 429-436. <http://dx.doi.org/10.1038/20859>
11. Hunter S.J., Goldobin D.S., Haywood A.M., Ridgwell A., Rees J.G. Sensitivity of the global submarine hydrate inventory to scenarios of future climate change. *Earth Planetary Sci. Lett.*, 2013, vol. 367, pp. 105-115. <http://dx.doi.org/10.1016/j.epsl.2013.02.017>
12. Henry W. III. Experiments on the quantity of gases absorbed by water, at different temperatures, and under different pressures. *Phil. Trans. R. Soc.*, 1803, vol. 93, pp. 29-43. <http://dx.doi.org/10.1098/rstl.1803.0004>
13. Pierotti R.A. A scaled particle theory of aqueous and nonaqueous solutions. *Chem. Rev.*, 1976, vol. 76, pp. 717-726. <http://dx.doi.org/10.1021/cr60304a002>
14. Baranenko V.I., Sysoev V.S., Fal'kovskii L.N., Kirov V.S., Piontkovskii A.I., Musienko A.N. The solubility of nitrogen in water. *At. Energy*, 1990, vol. 68, pp. 162-165. <http://dx.doi.org/10.1007/bf02069879>
15. Baranenko V.I., Fal'kovskii L.N., Kirov V.S., Kurnyk L.N., Musienko A.N., Piontkovskii A.I. The solubility of oxygen and carbon dioxide in water. *At. Energy*, 1990, vol. 68, pp. 342-346. <http://dx.doi.org/10.1007/bf02074362>
16. Yamamoto S., Alcauskas J.B., Crozier T.E. Solubility of methane in distilled water and seawater. *J. Chem. Eng. Data*, 1976, vol. 21, pp. 78-80. <http://dx.doi.org/10.1021/je60068a029>
17. Verhallen P.T.H.M., Oomen L.J.P., van den Elsen A.J.J.M., Kruger J., Fortuin J.M.H. The diffusion coefficients of helium, hydrogen, oxygen and nitrogen in water determined from the permeability of a stagnant

- liquid layer in the quasi-steady state. *Chem. Eng. Sci.*, 1984, vol. 39, pp. 1535-1541. [http://dx.doi.org/10.1016/0009-2509\(84\)80082-2](http://dx.doi.org/10.1016/0009-2509(84)80082-2)
18. Sachs W. The diffusional transport of methane in liquid water: method and result of experimental investigation at elevated pressure. *J. Petrol. Sci. Eng.*, 1998, vol. 21, pp. 153-164. [https://doi.org/10.1016/S0920-4105\(98\)00048-5](https://doi.org/10.1016/S0920-4105(98)00048-5)
19. Zeebe R.E. On the molecular diffusion coefficients of dissolved CO₂, HCO₃⁻, and CO₃²⁻ and their dependence on isotopic mass. *Geochim. Cosmochim. Acta*, 2011, vol. 75, pp. 2483-2498. <https://doi.org/10.1016/j.gca.2011.02.010>
20. Yerushov E.D. *General geocryology*. Cambridge University Press, 1998. 580 p. <https://doi.org/10.1017/CBO9780511564505>
21. Gregg S.J., Sing K.S.W. *Adsorption, surface area and porosity*. Academic Press, 1982. 303 p.
22. Bird R.B., Stewart W.E., Lightfoot E.N. *Transport phenomena*. Wiley, 2007. 928 p.
23. Frenkel J. *Kinetic theory of liquids*. Dover Publications, 1955. 488 p.
24. Maryshev B.S., Goldobin D.S. Accumulation of gases dissolved in water saturating a nonisothermal porous massif in the presence of water freezing zones. *IOP Conf. Ser.: Earth Environ. Sci.*, 2018, vol. 193, 012044. <https://doi.org/10.1088/1755-1315/193/1/012044>

The authors declare no conflict of interests.

The paper was received on 08.11.2021.

The paper was accepted for publication on 19.11.2021.